

A COMPACT STACKED BIDIRECTIONAL ANTENNA FOR DUAL-POLARIZED WLAN APPLICATIONS

Tianyu Jia^{1, 2} and Xiuping Li^{1, 2, *}

¹School of Electronic Engineering, Beijing University of Posts and Telecommunications, Beijing 100876, China

²State Key Laboratory of Millimeter Waves, Southeast University, Nanjing 210096, China

Abstract—A compact stacked bidirectional antenna is presented for dual-polarized 2.4 GHz WLAN applications in this paper. The antenna consists of an orthogonal coupling feed driver and stacked director array, with the overall size $50 \times 50 \times 160 \text{ mm}^3$. Dual-polarization is excited by the orthogonal coupling lines, and the director array contributes to the bidirectional radiation. Both the coupling feed driver and directors are printed on FR4 substrate and supported by plastic pillars. The measured bandwidth of the two ports are 2.33–2.62 GHz (11.8%) and 2.32–2.64 GHz (13%) under the condition of VSWR less than 2. The isolation between two ports is lower than -20 dB . The peak gains along one radiation direction are 9.65 dBi and 9.30 dBi for each port, with highly symmetric bidirectional beam pattern. The proposed antenna is compact and suitable for dual-polarized bidirectional 2.4 GHz WLAN applications.

1. INTRODUCTION

With the rapid development of wireless communications, fast expansion of wireless services, and increase of mobile subscribers, channel capacity is becoming more and more critical. Research work has focused on frequency reuse and polarization diversity by using two orthogonal polarizations [1–6]. Antennas with polarization diversity are widely studied and adopted in WLAN application [3, 4]. They are able to provide double transmission channels and increase channel capacity. To fulfill the dual-polarization, orthogonal coupling feeding is often adopted for its simple structure and ease of fabrication [3–6].

Received 22 August 2013, Accepted 22 September 2013, Scheduled 24 September 2013

* Corresponding author: Xiuping Li (xpli@bupt.edu.cn).

In some antennas [3, 4], special shaped slots are designed between the orthogonal feed lines and the radiation patch to guarantee the dual-polarization, while direct coupling feed to the patch can also achieve good performance [6]. In the proposed antenna, we adopted the direct coupling feed method, in which the orthogonal feeding lines could directly couple to the radiation directors.

For some specific services where the mobile users move along the straight roads such as highways, railways and tunnels, bidirectional antennas are especially preferred to be used in order to maximize the link efficiency [7–14]. The typical bidirectional antenna was accomplished by installing two unidirectional antennas in the opposite directions [7], but the directivity was not high, and the design was complicated. Researchers also proposed some compact planar bidirectional antennas, while the gain was limited by the substrate [8, 9]. In recent years, multilayered disk array structure (MDAS) or stacked director structure has been frequently adopted along the propagating direction to achieve unidirectional [5, 6] or bidirectional radiation [12–14]. In this article, the stacked director array along two radiation directions is adopted in the proposed antenna for bidirectional radiation.

Most previous dual-polarized antennas were designed to achieve only unidirectional radiation [5, 6], while most previous bidirectional antennas were single polarization [12–14]. In this paper, the proposed stacked antenna can achieve both dual-polarization and bidirectional radiation characteristics. The antenna structure is compact and suitable for bidirectional dual-polarized 2.4 GHz WLAN applications.

The organization of this article is as follows. In Section 2, we introduce the traditional Yagi-Uda antenna first and then propose the bidirectional Yagi antenna. Section 3 shows the proposed stacked bidirectional antenna structure based on the bidirectional Yagi antenna. Section 4 shows the antenna working principle and key parameter analysis. The experimental results of the fabricated prototype are given in Section 5. Finally, Section 6 gives the conclusions.

2. BIDIRECITONAL YAGI ANTENNA

Yagi-Uda antenna is the most common directional radiator which is widely studied [15–23] and can be applied in several frequency bands, such as VHF, UHF and even higher ranges. The traditional Yagi-Uda antenna normally consists of three parts: a driven element, reflector and a series of directors, as shown in Figure 1. Yagi-Uda antenna can achieve good unidirectional radiation and is widely used as a home

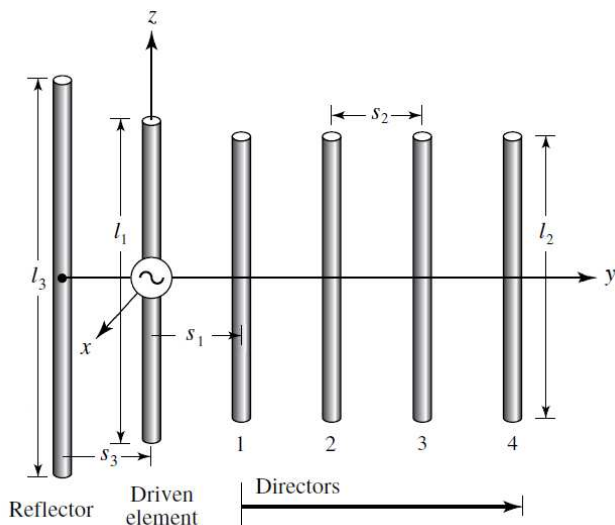


Figure 1. Geometry of the traditional Yagi-Uda antenna. [24] $l_1 \approx 0.42\lambda$, $l_2 \approx 0.36\lambda$, $s_1 = s_2 \approx 0.15\lambda$, $l_3 \approx 0.48\lambda$, $s_3 \approx 0.22\lambda$.

TV antenna. Typically, the driven element is resonant with its length slightly less than $\lambda/2$ (usually $0.45\text{--}0.49\lambda$) whereas the lengths of the directors should be about 0.4 to 0.45λ . The optimum spacing between the directors is normally 0.3 to 0.4λ , with the distance from driven element to reflector around 0.25λ [24].

With the good directional radiation characteristic of Yagi-Uda antenna, it is a good choice to achieve our bidirectional radiation target. The simplest way is combining two reversed single Yagi-Uda antennas and feeding them respectively. However, this method increases the overall size by at least two times and more complex for feeding, without considering the mutual coupling between two antennas. For compact fabrication and bidirectional applications, we improve the traditional Yagi-Uda antenna by removing the reflector and arranging the directors along both sides of the driven element, as shown in Figure 2. In the proposed structure, only driven element and directors are needed, with smaller size than the combination of two single Yagi-Uda antennas.

For comparing the performance of the traditional Yagi-Uda and the proposed bidirectional antenna, we build an optimum Yagi-Uda antenna with four directors and a bidirectional Yagi antenna with eight directors. The dimensions of driven element, director length and director spacing maintain the same in both two structures.

The performances of these two antennas are compared in Figure 3.

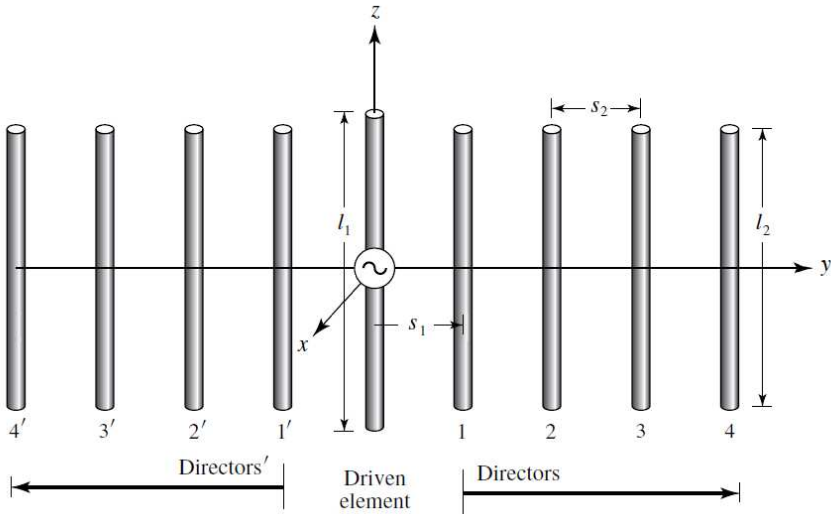


Figure 2. Geometry of the bidirectional Yagi antenna.

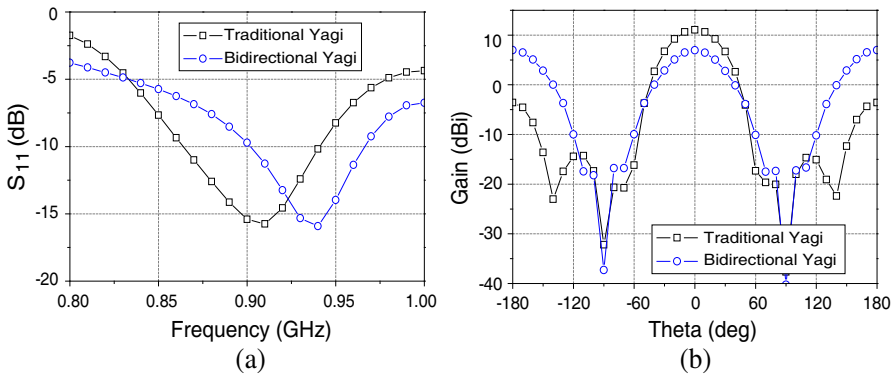


Figure 3. Performance comparison between the traditional and bidirectional Yagi antenna. (a) S_{11} . (b) Radiation gain.

As shown in Figure 3(a), the bidirectional antenna has a frequency offset around 30 MHz (3.3%) from the original Yagi antenna. This small offset can be easily adjusted by optimizing the length of the driven element and spacing between driven element and the directors. However, the maximum gain decreases with removing the reflectors, from the original around 11 dBi to bidirectional 7 dBi. Thus, some tradeoff between high gain and compact structure should be considered

according to the practical demands. For our research, a compact structure is preferred, and the bidirectional Yagi antenna structure is adopted for the following design.

3. ANTENNA CONFIGURATION

Based on the bidirectional Yagi antenna mentioned in the last section, we propose a stacked bidirectional antenna in this section. The proposed antenna consists of two parts, the coupling feed driver and stacked director array. The configuration of the coupling feed driver is shown in Figure 4. The coupling feed driver comprises two orthogonal folded feed lines, which are printed on the top and bottom layers of $50 \times 50 \text{ mm}^2$ FR4 substrate (thickness = 0.8 mm, $\epsilon_r = 4.4$, $\tan \delta = 0.02$). The orthogonal feed lines contribute to the vertical and horizontal polarization modes, respectively. The width of the feeding line is W and the length about $L_1 + L_2$. The metal ground area is $G_1 \times G_2$, which is printed on the bottom layer. The total electrical length of the feeding line can be treated as $L_1 + L_2 - G_1$, which equals about $\lambda_g/2$ at 2.45 GHz. The design of folded feed lines can avoid overlapping area between top and bottom layers and maintain electrical length for target resonant frequency. In that case, we can improve the isolation between two ports and also make the section area smaller. In addition, there are four holes in the corner with diameter R for the connection with other components.

The proposed bidirectional antenna combines the coupling feed driver and stacked director array, as shown in Figure 5. The stacked director array consists of four square directors along each radiation

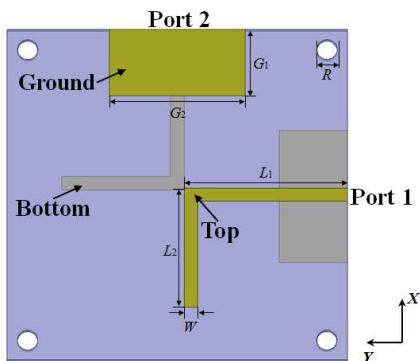


Figure 4. Configuration of the coupling feed driver. $L_1 = 24 \text{ mm}$, $L_2 = 18 \text{ mm}$, $W = 2 \text{ mm}$, $G_1 = 10 \text{ mm}$, $G_2 = 20 \text{ mm}$, $R = 3 \text{ mm}$.

direction, with all printed in the center of the same $50 \times 50 \text{ mm}^2$ FR4 substrates. The side length of the first director from coupling driver is D_1 , while the side length increases by Dis from the nearest one to the farthest director from the feed driver. Dis is adopted as 5 mm in the proposed antenna, and the side lengths of the other three directors are D_2, D_3, D_4 , respectively. The increase of director length is valuable to improving the gain performance, which will be further discussed in the next section. The stacked director array is symmetrically distributed, and the metal directors face away for the driver. The spacing between the coupling feed driver and the first director is S_1 , while the spacing between other directors is S_2 , about $\lambda_0/5$.

The fabricated antenna is shown in Figure 6. Both the coupling feed driver and stacked directors are printed on $50 \times 50 \text{ mm}^2$ FR4 substrates. Plastic pillars with the length of S_1 and S_2 are chosen to support all these substrates. The overall size of the proposed antenna is $50 \times 50 \times 160 \text{ mm}^3$.

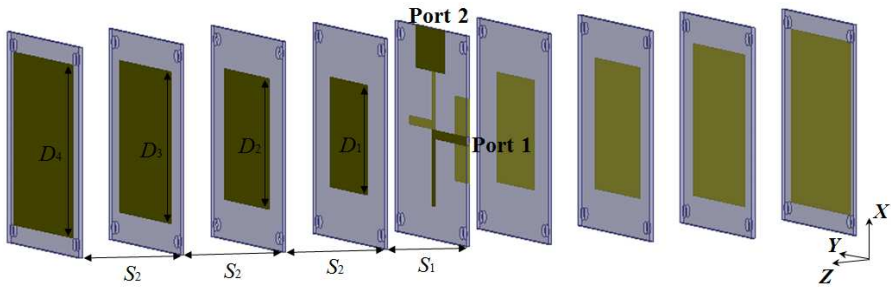


Figure 5. Configuration of the proposed bidirectional antenna. $S_1 = 5 \text{ mm}$, $S_2 = 25 \text{ mm}$, $D_1 = 26 \text{ mm}$, $D_2 = 31 \text{ mm}$, $D_3 = 36 \text{ mm}$, $D_4 = 41 \text{ mm}$, $Dis = D_4 - D_3 = D_3 - D_2 = D_2 - D_1 = 5 \text{ mm}$.

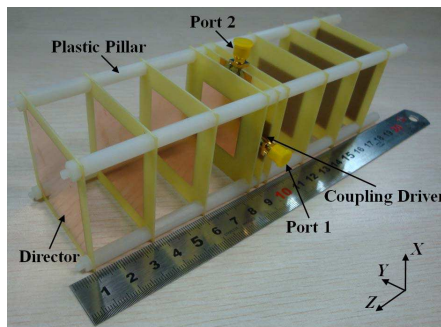


Figure 6. Photograph of the fabricated antenna prototype.

4. STUDIES OF THE PROPOSED ANTENNA

4.1. Current Distributions

In this section, the simulated current distributions on metal surfaces are provided to analyze the antenna working principle. The simulated current distributions on the coupling feed lines are given in Figure 7. It is observed that when feeding from port 1, vertical polarization mode is excited, while exciting port 2 contributes to the horizontal polarization mode. When port 1 and port 2 are fed together, they will couple to the directors simultaneously, and the dual-polarization radiation can be obtained.

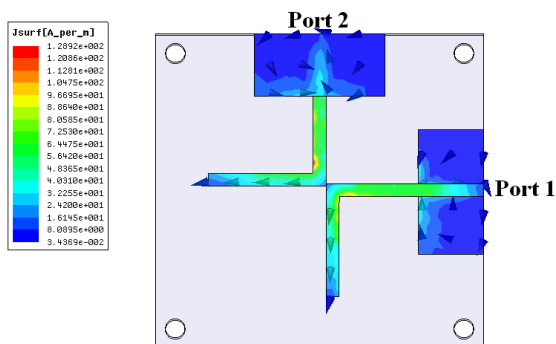


Figure 7. Simulated current distributions on the coupling line at 2.45 GHz.

Figure 8 shows the current distribution on the director surface when feeding from port 1 and port 2, respectively. The $\lambda_0/5$ spacing between neighboring directors causes the phase difference around 180° and achieves nice propagation. The distal directors can be regularly excited and improve peak gain along both sides. Besides, the current vectors show again that port 1 is responsible for vertical polarization, and port 2 contributes to the horizontal polarization mode.

4.2. Parametric Analysis

In this section, the key parameters of the proposed antenna will be studied. According to the simulations, we find that the coupling driver dimensions affect the antenna resonance notably and that the director size has much impact on the maximum gain.

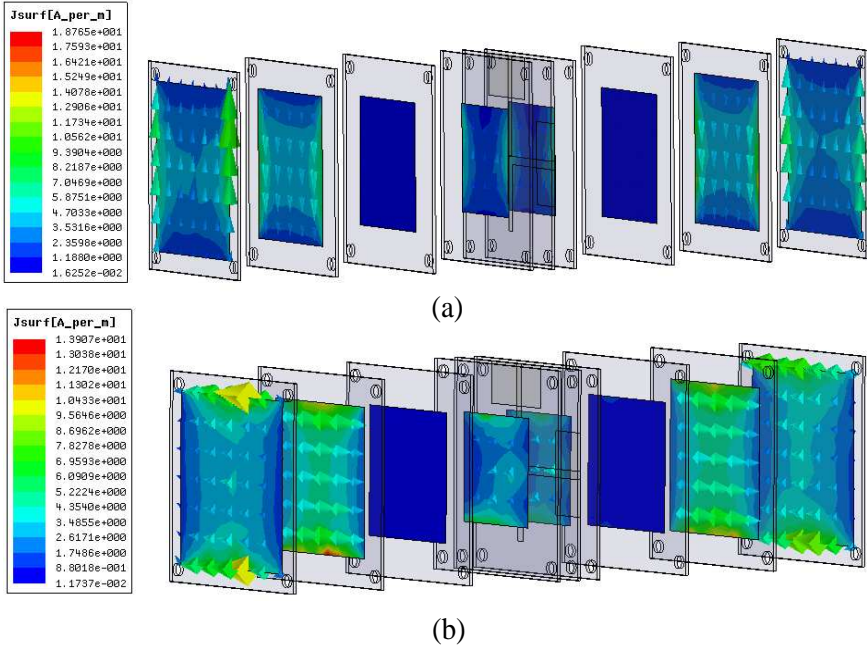


Figure 8. Simulated current distributions on the director surface at 2.45 GHz when feeding at (a) Port 1 and (b) Port 2.

The key parameters for the resonant frequency are the feeding line length L_2 and director spacing S_1 , as shown in Figure 9. The simulations show that the increasing either L_2 or S_1 will extend the equivalent electrical length and decrease the resonant frequency. L_1 can also tune the resonance, while larger L_1 will create the overlap area between top and bottom layers and reduce the port isolation. Thus parameters L_2 and S_1 are the keys for us to adjust to the target frequency.

The functions of the director spacing S_2 and director side length difference Dis to gain performance are shown in Figure 10. The simulated gain curves on the xz -plane are chosen for the comparison. In [4], the printed stacked antenna was studied and showed the optimum director spacing ranges from $\lambda_0/5$ to $\lambda_0/4$. In the proposed antenna, the director spacing is decided by parameter S_2 , which is 25 mm and around $\lambda_0/5$. In addition, the increasing trend of the director length can increase the maximum gain, which is decided by the parameter Dis , as shown in Figure 4(b). It is observed that when $Dis = 5$ mm, the max gain is nearly 10 dBi, while the gain decreases by 2 dBi as the $Dis = 4$ mm.

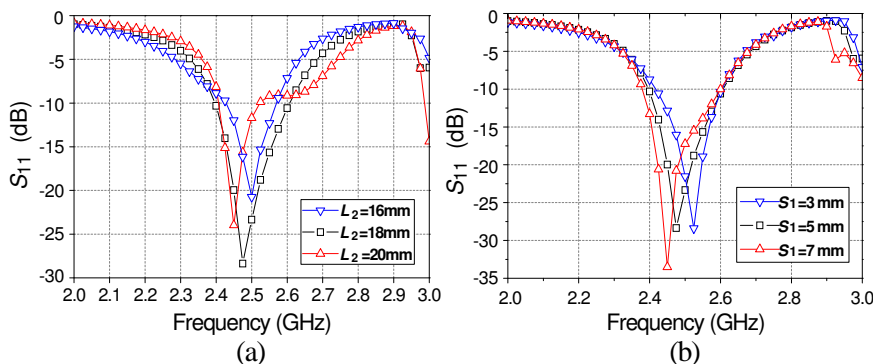


Figure 9. Simulated S_{11} with different dimensions at 2.45 GHz. (a) Coupling feed length L_2 . (b) Spacing between driven element and directors S_1 .

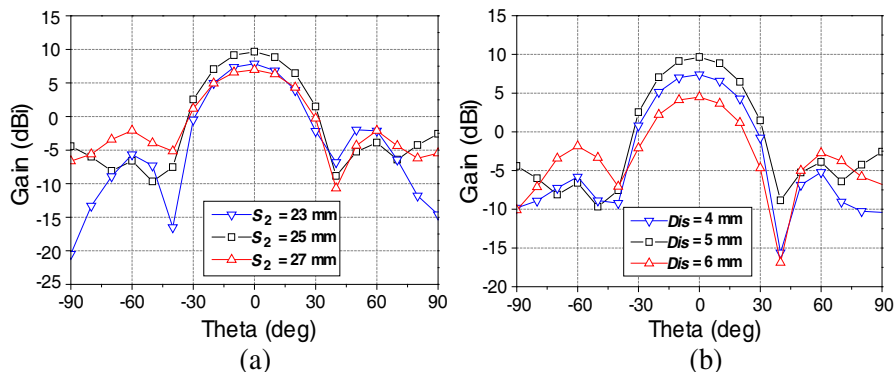


Figure 10. Simulated gain performance with different dimensions at 2.45 GHz. (a) Director length difference Dis . (b) Director spacing S_2 .

5. EXPERIMENTAL RESULTS

The experimental results of the proposed antenna are presented in this section. The simulated and measured S parameters results are given in Figure 11, with all the simulation results accomplished by *HFSS 13*. The measured bandwidth is 2.33–2.62 GHz (11.8%) for port 1 (vertical polarization) and 2.32–2.64 GHz (13%) for port 2 (horizontal polarization) under the condition of VSWR less than 2, respectively. Over the operating band, the isolation between two ports, S_{21} , is lower than -20 dB. As the two ports are symmetric by Z axis, S_{12} is equal to S_{21} in the proposed antenna. The measured and simulated results agree well.

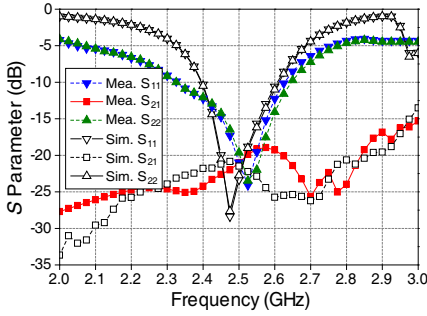


Figure 11. Simulated and measured S parameter results of the proposed antenna.

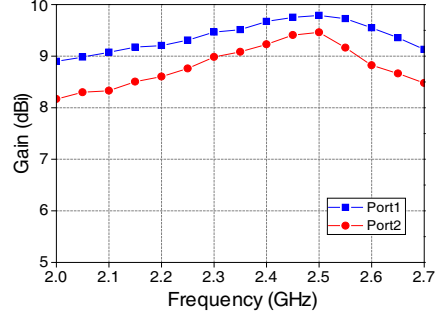


Figure 12. Measured gain along $+z$ axis when feeding from port 1 and port 2.

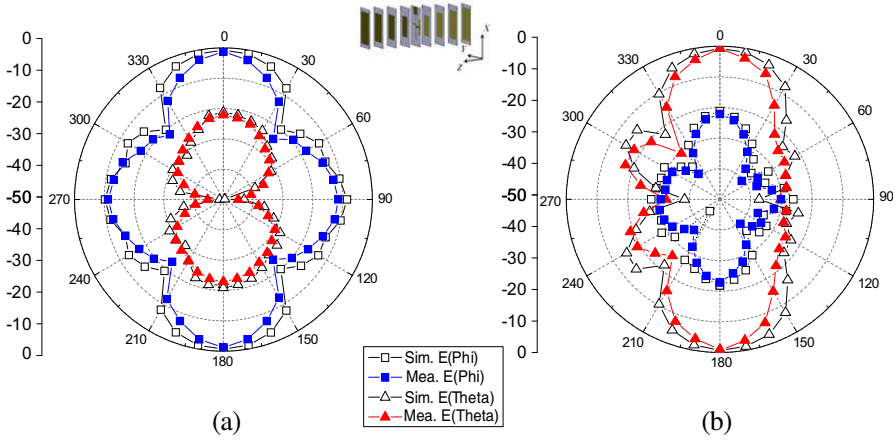


Figure 13. Measured and simulated radiation pattern: Feeding from port 1 at 2.45 GHz. (a) xz -plane. (b) yz -plane.

The measured gain values along $+z$ axis, when feeding from two ports separately, are presented in Figure 12. The measured gains were obtained using the gain transfer method, with a standard horn antenna used as a reference. It is found that the gain range for port 1 (vertical polarization) is about 9.2–9.6 dBi and for port 2 (horizontal polarization) about 8.9–9.3 dBi in the operating band (2.4–2.5 GHz). The difference of the peak gain value is mainly caused by the two coupling feed lines printed on the different layers of the substrate.

Figures 13 and 14 show the simulated and measured normalized radiation patterns at 2.45 GHz when feeding from port 1 and port 2,

respectively. *Phi* is the angle in *xz*-plane, while *Theta* is the reference angle in *yz*-plane. As shown in the figure, the vertical polarization is achieved when feeding from port 1 (*xz*-plane), while horizontal polarization is dominated when feeding from port 2 (*yz*-plane). The proposed antenna has a cross-polarization level of less than 20 dB below the co-polarization for both ports. Besides, these radiation pattern figures show a highly concentrated bidirectional beam pattern.

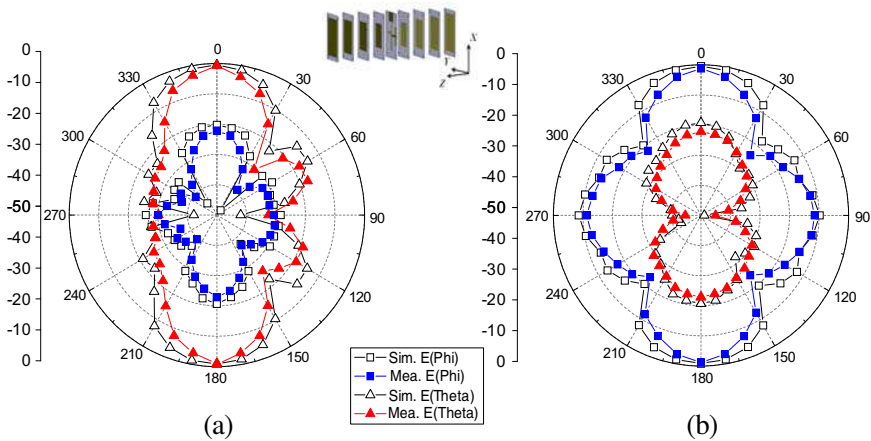


Figure 14. Measured and simulated radiation pattern: Feeding from port 2 at 2.45 GHz. (a) *xz*-plane. (b) *yz*-plane.

Table 1. The comparison with some previous directional antennas.

	Overall Size (mm ³)	Peak Gain (dBi)	Radiation Direction
Proposed Antenna	$0.41\lambda_0 \times 0.41\lambda_0 \times 1.31\lambda_0$	9.6	Bidirectional
Antenna in [10]	$\pi \times (1.93\lambda_0)^2 \times 1.26\lambda_0$	8.9	Bidirectional
Antenna in [13]	$\pi \times (0.61\lambda_0)^2 \times 2.15\lambda_0$	10.29	Bidirectional
Antenna in [6]	$0.96\lambda_0 \times 0.96\lambda_0 \times 1.13\lambda_0$	9.76	Unidirectional
Antenna in [12]	$\pi \times (0.75\lambda_0)^2 \times 1.34\lambda_0$	11.18	Unidirectional

The performance of the proposed bidirectional antenna is also compared with some previous directional antennas, as shown in Table 1. With the design of folded feeding line, the section area of the proposed antenna is compact. Besides, four directors along each radiation direction decrease the overall length. The proposed antenna is only around 9% of the bidirectional antenna in [13] and 21% of the unidirectional antenna in [6]. The antenna peak gain value is just slightly decreased but still acceptable with its compact size.

6. CONCLUSION

A compact stacked bidirectional antenna has been presented for dual-polarized 2.4 GHz WLAN applications in this article. The antenna consists of an orthogonal coupling feed driver and a stacked director array, with an overall size $50 \times 50 \times 160 \text{ mm}^3$. The measured bandwidths of the two polarizations are 2.33–2.62 GHz (11.8%) and 2.32–2.64 GHz (13%) under the condition of VSWR less than 2. The isolation between two ports is lower than -20 dB in the operating band. The peak gain values along one radiation direction are 9.65 dBi and 9.30 dBi for each port at 2.45 GHz, with highly symmetric bidirectional beam pattern. The measured and simulated results agree well. The proposed antenna is compact and can be a good candidate for dual-polarized bidirectional WLAN applications.

ACKNOWLEDGMENT

This work is supported by the projects 61072009 and 61372036 from the National Natural Science Foundation of China (NSFC), the 863 project 2011AA010201, Fundamental Research Funds for the Central Universities and the Fund of State Key Laboratory of Millimeter Waves, Southeast University (Grant No. K201209).

REFERENCES

1. Peng, H. L., W. Y. Yin, J. F. Mao, D. Huo, X. Hang, and L. Zhou, "A compact dual-polarized broadband antenna with hybrid beam-forming capabilities," *Progress In Electromagnetic Research*, Vol. 118, 253–271, 2011.
2. Secmen, M. and A. Hizal, "A dual-polarized wide-band patch antenna for indoor mobile communication applications," *Progress In Electromagnetic Research*, Vol. 100, 189–200, 2010.

3. Yen, L. K. and K. L. Wong, "Dual-polarized monopole antenna for WLAN application," *Antennas and Propagation Society International Symposium*, Vol. 4, 80–83, 2002.
4. Ezzeldin, A. S., S. I. Magdy, and K. A. Alaa, "Dual-polarized omnidirectional planar slot antenna for WLAN applications," *IEEE Trans. Antennas Propagat.*, Vol. 53, No. 9, 3093–3097, 2005.
5. Nepa, P., G. Manara, G. Tribellini, and S. Cioci, "A wide-band dual-polarized stacked patch antenna," *IEEE Antennas and Wireless Propagation Letters*, Vol. 6, 141–143, 2007.
6. Kramer, O., T. Djerafi, and K. Wu, "Vertically multilayer-stacked Yagi antenna with single and dual polarizations," *IEEE Trans. Antennas Propagat.*, Vol. 58, No. 4, 1022–1030, 2010.
7. Arai, H., K. Kohzu, T. Mukaiyama, and Y. Ebine, "Bi-directional notch antenna with parasitic elements for tunnel booster system," *Antennas and Propagation Society International Symposium*, Vol. 4, 2218–2221, 1997.
8. Iwasaki, H., "Slot-coupled back-to-back microstrip antenna with an omni- or a bi-directional radiation pattern," *IEE Proceedings, Microwave, Antennas and Propagation*, Vol. 146, 219–223, 1999.
9. Lamultree, S. and C. Phongcharoenpanich, "Bidirectional ultra-wideband antenna using rectangular ring fed by stepped monopole," *Progress In Electromagnetic Research*, Vol. 85, 227–242, 2008.
10. Li, X., L. Yang, S. X. Gong, and Y. J. Yang, "Bidirectional high gain antenna for WLAN applications," *Progress In Electromagnetics Research Letters*, Vol. 6, 99–106, 2009.
11. Mahatthanajatuphat, C., P. Akkaraekthalin, S. Saleekaw, and M. Krairiksh, "A directional multiband antenna with modified fractal slot fed by CPW," *Progress In Electromagnetic Research*, Vol. 95, 59–72, 2009.
12. Eom, S. Y., S. K. Kim, and J. G. Yook, "Multilayered disk array structure surrounded by a dielectric ring for shaping a flat-topped radiation pattern," *Antennas and Wireless Propagation Letters*, Vol. 7, 374–376, 2008.
13. Eom, S. Y., L. Minz, M. K. Joung, and C. JaeIck, "High gain bidirectional microstrip dipole antenna," *2011 IEEE International Conference on Ultra-Wideband (ICUWB)*, 21–24, 2011.
14. Batgerela, A., J. I. Choib, and S. Y. Eomb, "High-gain bidirectional MDAS antenna design excited by stacked-microstrip dipole," *Journal of Electromagnetic Waves and Applications*, Vol. 26, Nos. 11–12, 1412–1422, 2012.

15. Yagi, H., "Beam transmission of ultra short waves," *Proceedings of the IEEE*, Vol. 85, No. 11, 1864–1874, 1997.
16. Ehrenspeck, H. W. and H. Poehler, "A new method for obtaining maximum gain from Yagi antennas," *IRE Trans. Antennas Propagat.*, Vol. 7, 379–386, 1959.
17. Thiele, G. A., "Analysis of Yagi-Uda type antennas," *IEEE Trans. Antennas Propagat.*, Vol. 17, No. 1, 24–31, 1969.
18. Cheng, D. K. and C. A. Chen, "Optimum spacings for Yagi-Uda arrays," *IEEE Trans. Antennas Propagat.*, Vol. 21, No. 5, 615–623, 1973.
19. Chen, C. A. and D. K. Cheng, "Optimum element lengths for Yagi-Uda arrays," *IEEE Trans. Antennas Propagat.*, Vol. 23, No. 1, 8–15, 1975.
20. Sun, B. H., S. G. Zhou, Y. F. Wei, and Q. Z. Liu, "Modified two-element Yagi-Uda antenna with tunable beams," *Progress In Electromagnetics Research*, Vol. 100, 175–187, 2010.
21. Majid, H. A., M. K. A. Rahim, M. R. Hamid, and M. F. Ismail, "Frequency and pattern reconfigurable Yagi antenna," *Journal of Electromagnetic Waves and Applications*, Vol. 26, Nos. 2–3, 379–389, 2012.
22. Lin, S., G. L. Huang, R. N. Cai, and J. X. Wang, "Novel printed Yagi-Uda antenna with highgain and broadband," *Progress In Electromagnetics Research Letters*, Vol. 20, 107–117, 2011.
23. Mohammed, J. R., "Design of printed yagi antenna with additional driven element for WLAN applications," *Progress In Electromagnetics Research C*, Vol. 37, 67–81, 2013.
24. Balanis, C. A., *Antenna Theory: Analysis and Design*, 3rd Edition, John Wiley & Sons, Hoboken, New Jersey, 2005.